

Lys11-linked ubiquitin chains adopt compact conformations and are preferentially hydrolyzed by the deubiquitinase Cezanne

Supplementary Material

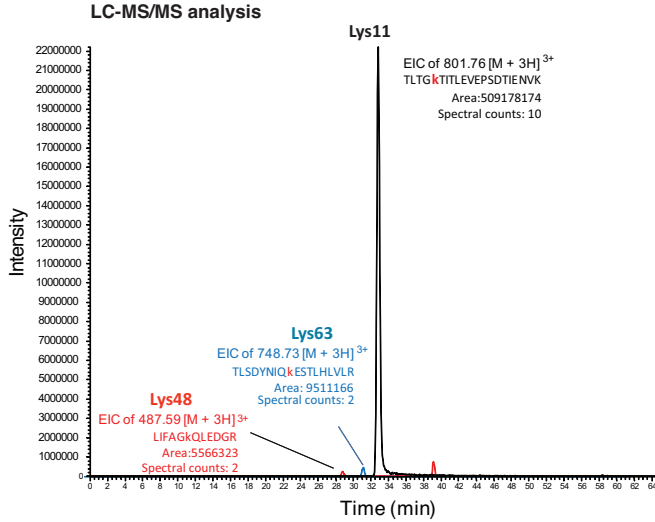
Anja Bremm, Stefan M.V. Freund and David Komander*

Medical Research Council Laboratory of Molecular Biology, Hills Road,
Cambridge, UK

* Correspondence should be addressed to: David Komander, MRC Laboratory of Molecular Biology, Protein and Nucleic Acid Chemistry Division, Hills Road, Cambridge, CB2 0QH, UK. Email: dk@mrc-lmb.cam.ac.uk, Tel: +44 1223 402300, Fax: +44 1223 412178

Running title: Lys11-linked polyubiquitin chains

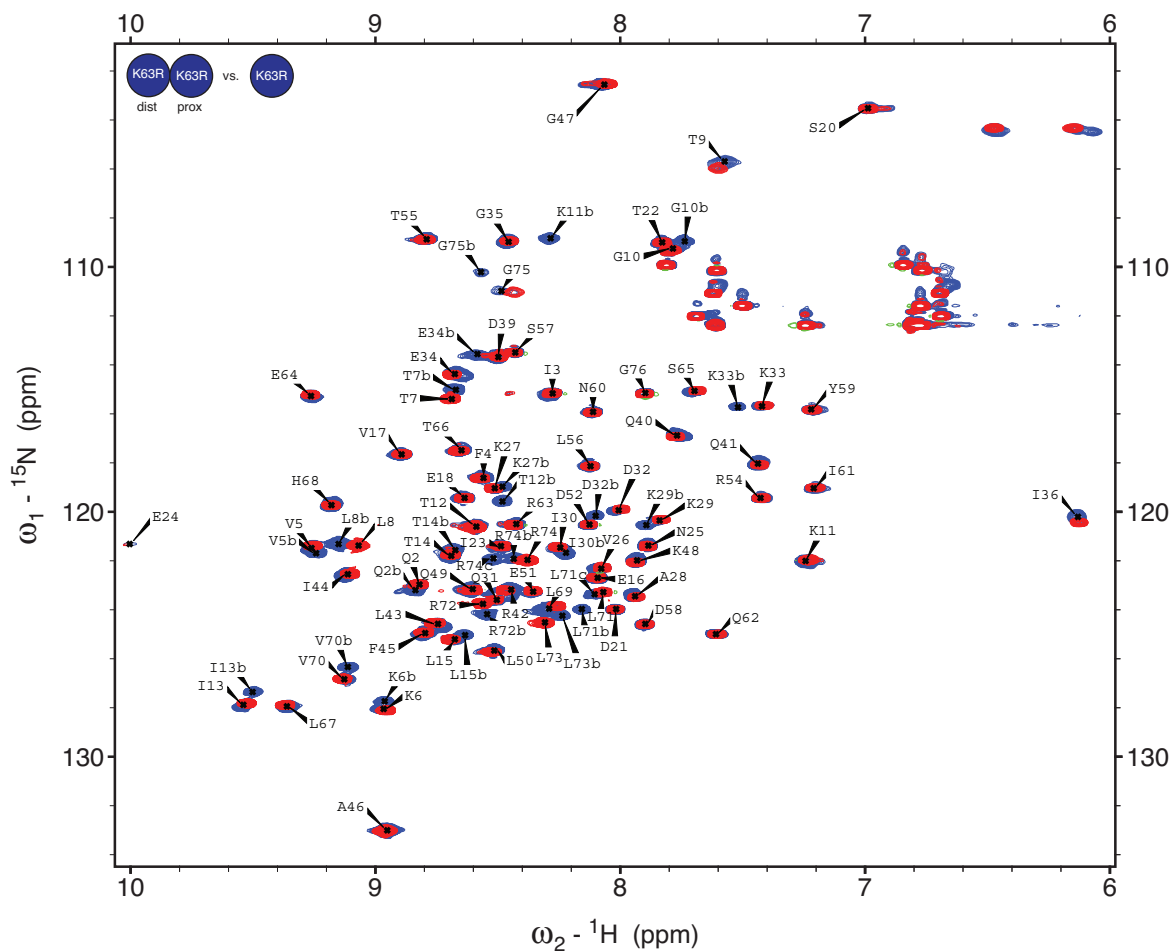
Supplementary Figure 1



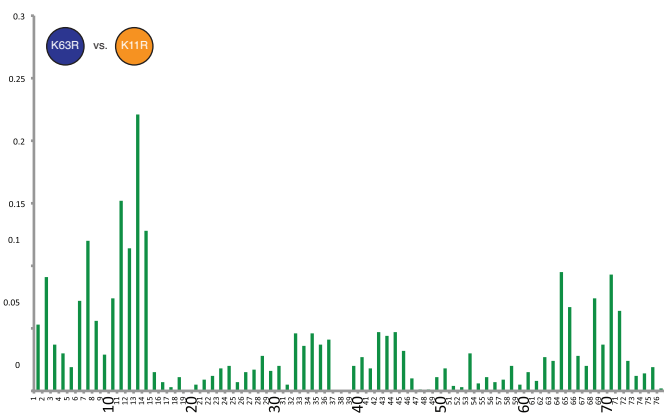
Supplementary Figure 1: LC-MS/MS analysis of Lys11-linked diubiquitin.

Extracted ion chromatograms of GlyGly-modified peptides produced after trypsin digestion of ubiquitin dimers assembled by UBE2S. Even though GlyGly-modifications were detected at three different lysine residues, namely Lys11(black trace), Lys48 (red trace) and Lys63(blue trace), the integrated peak areas and the spectral counts indicate that the Lys11-linkage is predominant.

a



b

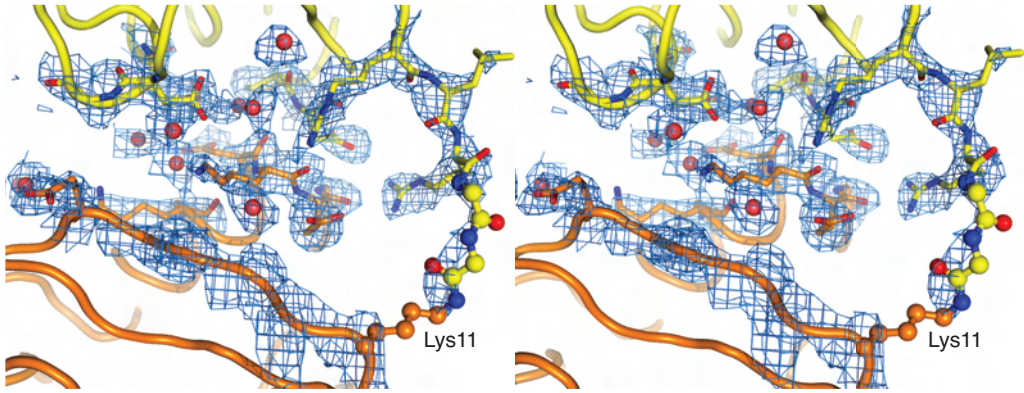


Supplementary Figure 2: NMR solution studies.

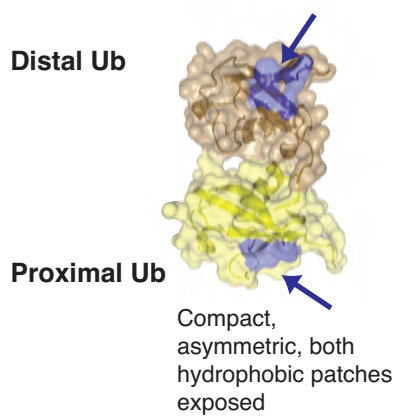
(a) Assignment of Lys11-linked diubiquitin from ^{13}C , ^{15}N -labeled K63R ubiquitin. The spectra shown derive from a K63R monoubiquitin (red) overlaid with K11-linked diubiquitin assembled from K63R ubiquitin (blue). In the diubiquitin sample all interface residues show a doubled signal, as the interface is asymmetric. In perturbed resonances, 50% of the signal overlaps with the non-perturbed conformation as found in monoubiquitin, while the remaining 50% is shifted (labeled with b). For Leu71 and Arg74, the monoubiquitin resonance is distinct from both resonances derived from the diubiquitin, and these are labeled L71b/L71c and R74b/R74c respectively. (b) Chemical perturbation difference map obtained from comparison of resonances from K11R monoubiquitin and K63R monoubiquitin. Note that the differences are due to both mutations in the sample.

Supplementary Figure 3

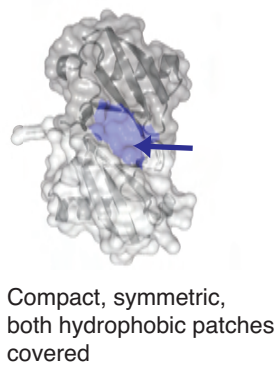
a Simulated annealing OMIT map



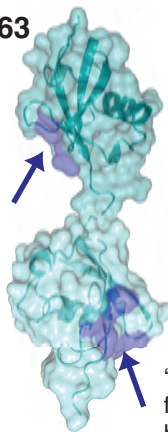
b Lys11



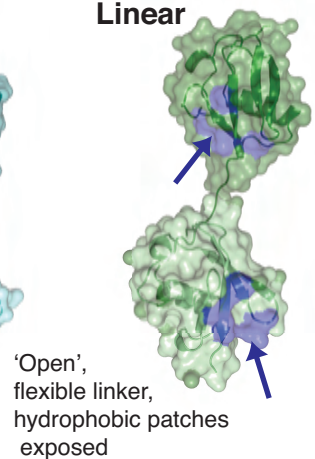
c Lys48



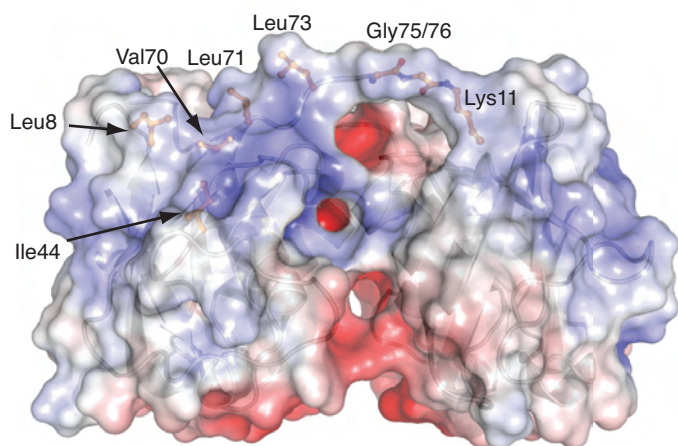
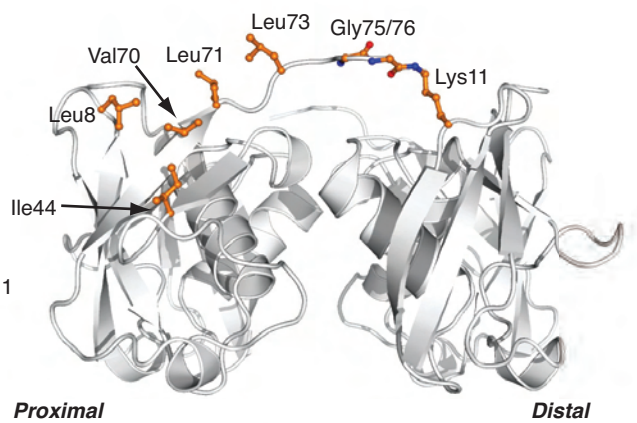
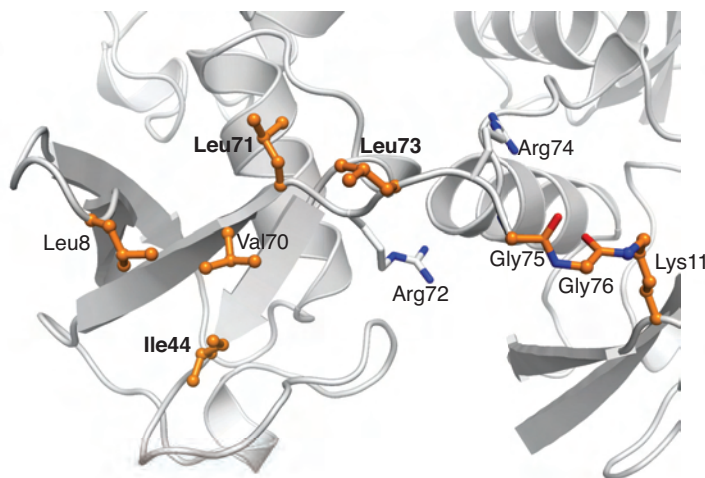
d Lys63



e Linear



f

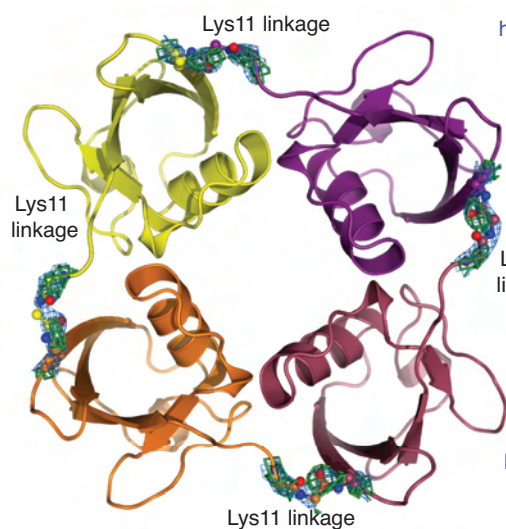


Supplementary Figure 3: Crystal structure of Lys11-linked diubiquitin.

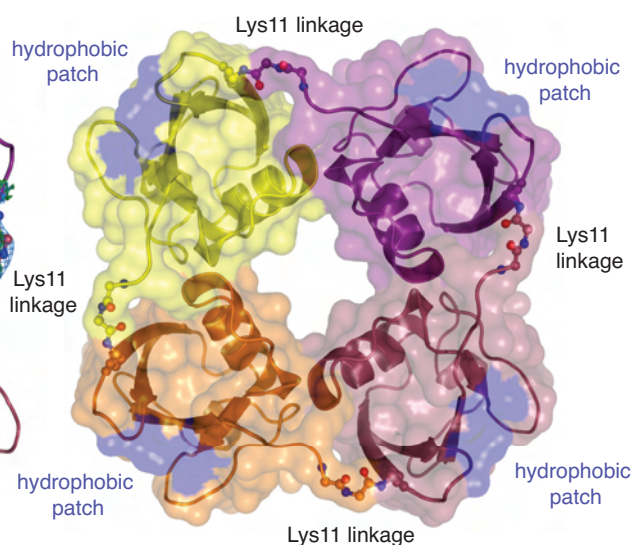
(a) Stereo-representation of the crystallographic Lys11-diubiquitin interface as in **Fig. 2c**. A simulated annealing OMIT map, calculated with Phenix⁶ and contoured at 1σ , covers the residues at the interface. **(b-e)** A surface representation of crystal structures from differentially linked diubiquitin shows their distinct conformations. The respective proximal and distal ubiquitin moieties are indicated, and the position of the hydrophobic patch is shown in blue on the surface and indicated by arrows. **(b)** Crystal structure of Lys11-linked diubiquitin determined in this study (see **Fig. 3b**). **(c)** Crystal structure of Lys48-linked diubiquitin, in which the ubiquitin moieties interact via their hydrophobic patches (pdb-id 1aar, ¹⁷). **(d)** Crystal structure of the extended and flexible Lys63-linked diubiquitin, which does not contain an interface between ubiquitin moieties (pdb-id 2jf5, ¹). **(e)** Crystal structure of linear diubiquitin, which crystallizes in the same setting as Lys63-linked diubiquitin, adopting the same 'open' conformation (pdb-id 2w9n, ¹). **(f)** In the crystal structure, the hydrophobic surface in Lys11-linked chains is extended by Leu71 and Leu73, which are exposed as Arg72/Arg74 participate in the interface. An electrostatic surface potential is shown on the Lys11-linked ubiquitin dimer, where blue colors indicate a positive partial charge, red colors negative charge and white uncharged regions. The hydrophobic surface patch residues are labeled and indicated by arrows.

Supplementary Figure 4

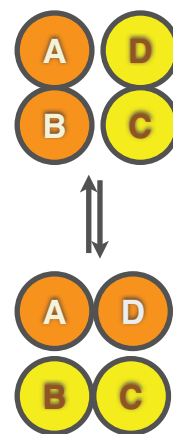
a Dimer interactions



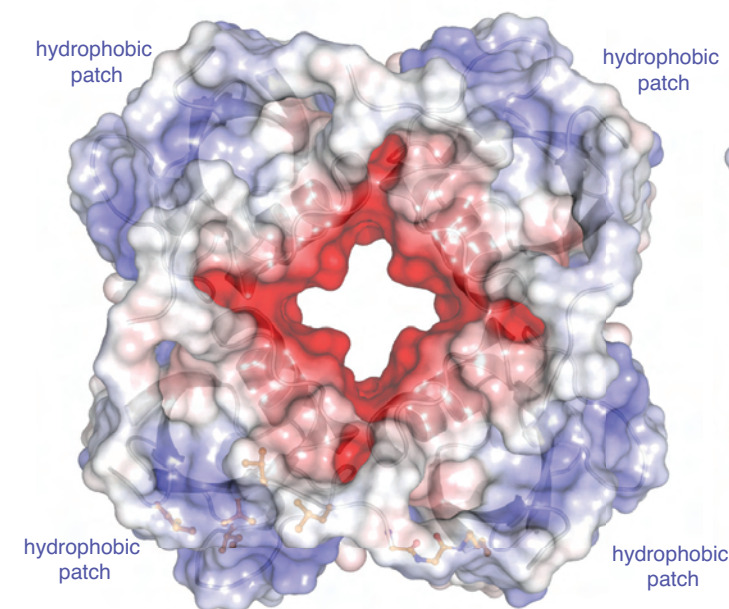
b Exposed Ile44 patch



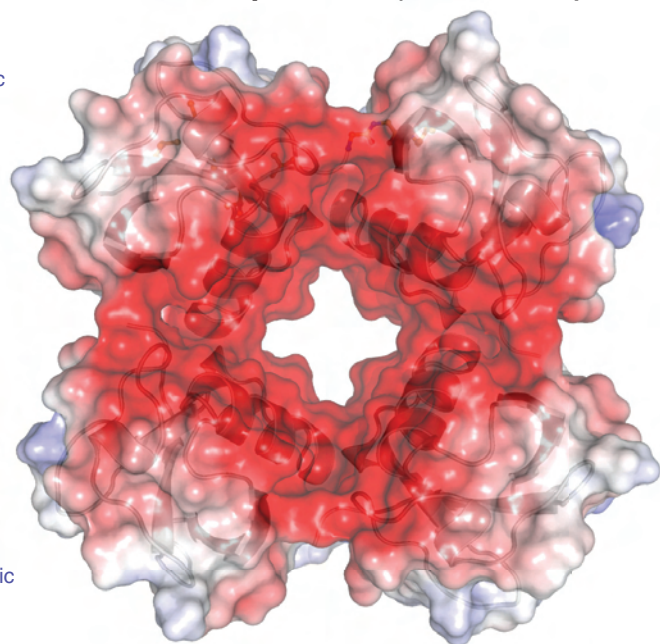
c Linkage ambiguity



d Electrostatic potential (from above)

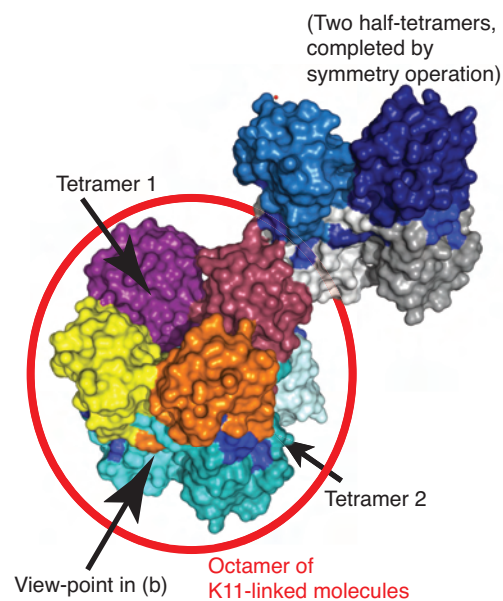
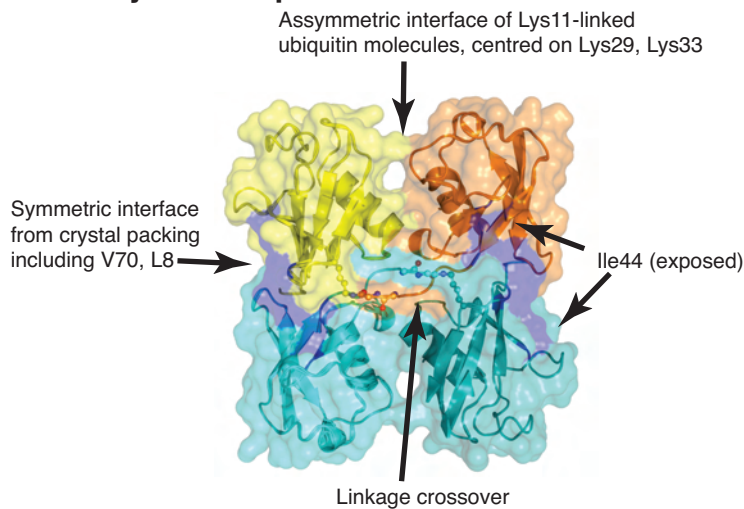
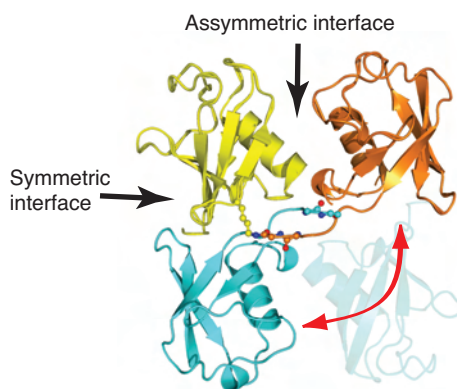


e Electrostatic potential (from below)



Supplementary Figure 4: Dimer interactions of Lys11-linked diubiquitin.

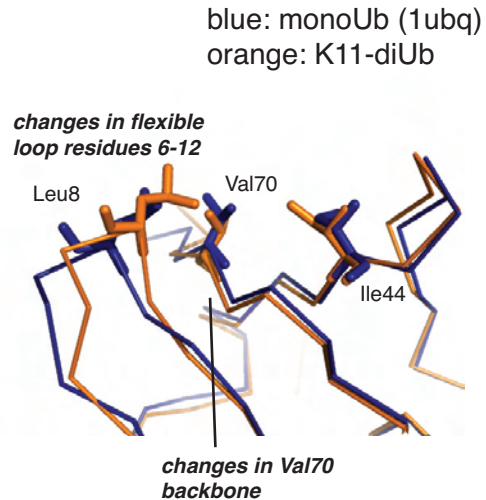
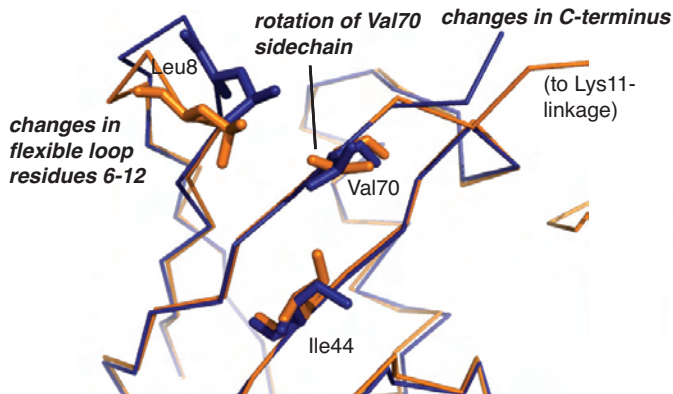
(a) Lys11-linked diubiquitin interactions in the crystal reveal a symmetric model for Lys11-linked tetramers, in which the isopeptide linkages are exposed. $2|F_o| - |F_c|$ electron density at 1σ in blue, and a simulated annealing omit map at 1σ in green is shown for the linking residues (Gly75, Gly76, Lys11). (b) The hydrophobic patch in a Lys11-linked tetramer points towards the perimeter of the wheel, and is solvent exposed and poised for interaction. (c) The crystal represents an average of two packing arrangements, resulting in linkage ambiguity. (d, e) Electrostatic surface potential of the tetramer model as derived from the crystal structure, viewed from above (d) and below (e). The linkage residues form a hydrophobic crown on the tetramer, where they are involved in further crystal contacts (see **Supp Fig. 5**), while core of the tetramer is negatively charged.

a Asymmetric unit**b Two Lys11-compatible interfaces****c two conformations for diubiquitin****Supplementary Figure 5: A putative second symmetric Lys11-compatible interface in the Lys11-diubiquitin crystal structure.**

(a) The ubiquitin content of the asymmetric unit shows higher order complexes adopted by Lys11-linked diubiquitin. The highest-order organizing principle is an octamer of ubiquitin molecules, consisting of two tetrameric assemblies mediated by the interfaces as described in the main text (see **Fig. 5** and **Supp. Fig. 4**). Two tetramers stack ‘head-on-head’ to form a symmetric octameric barrel-shaped structure. This results in a further symmetric contact interface for each ubiquitin molecule with a neighboring moiety. (b) In the symmetric ‘stacking’ interface between tetramers, interactions form through an interface containing Leu8 and Val70. The C-terminus of ubiquitin molecules is spatially close to the Lys11 side chain, potentially allowing isopeptide bond formation, although in the crystal structure, linkages between stacking molecules are not defined by electron density. (c) Perturbed residues in solution could originate from an interconversion between the two putative interfaces in solution.

Supplementary Figure 6

Perturbations at Leu8, Val70

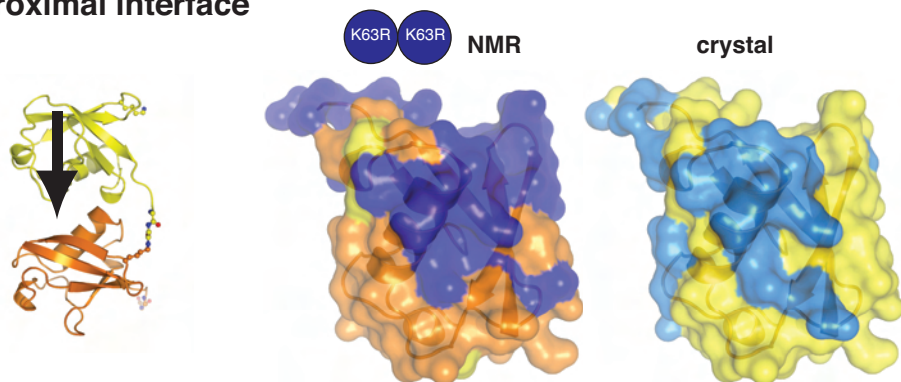


Supplementary Figure 6: Alternative explanation for observed perturbations in Leu8 and Val70.

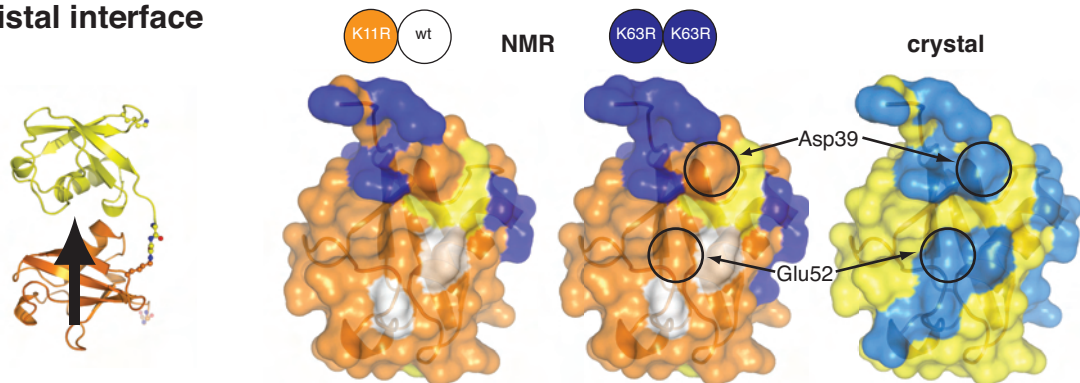
The structure of monoubiquitin (blue, pdb-id 1ubq) was superimposed on the distal moiety of the Lys11-linked diubiquitin structure (orange). Two different views are shown, and residues Leu8, Val70 and Ile44 are shown as stick representations. The main chain of the ubiquitin flexible loop containing Leu8, and of the ubiquitin C-terminus including Val70, differ significantly, potentially accounting for chemical shift perturbations. Hence, it is possible that perturbations at Val70/Leu8 arise from the isopeptide linkage at Gly76, which may relay conformational changes towards Val70, and Leu8 in the ubiquitin flexible loop may adjust in concert.

Supplementary Figure 7

a Proximal interface



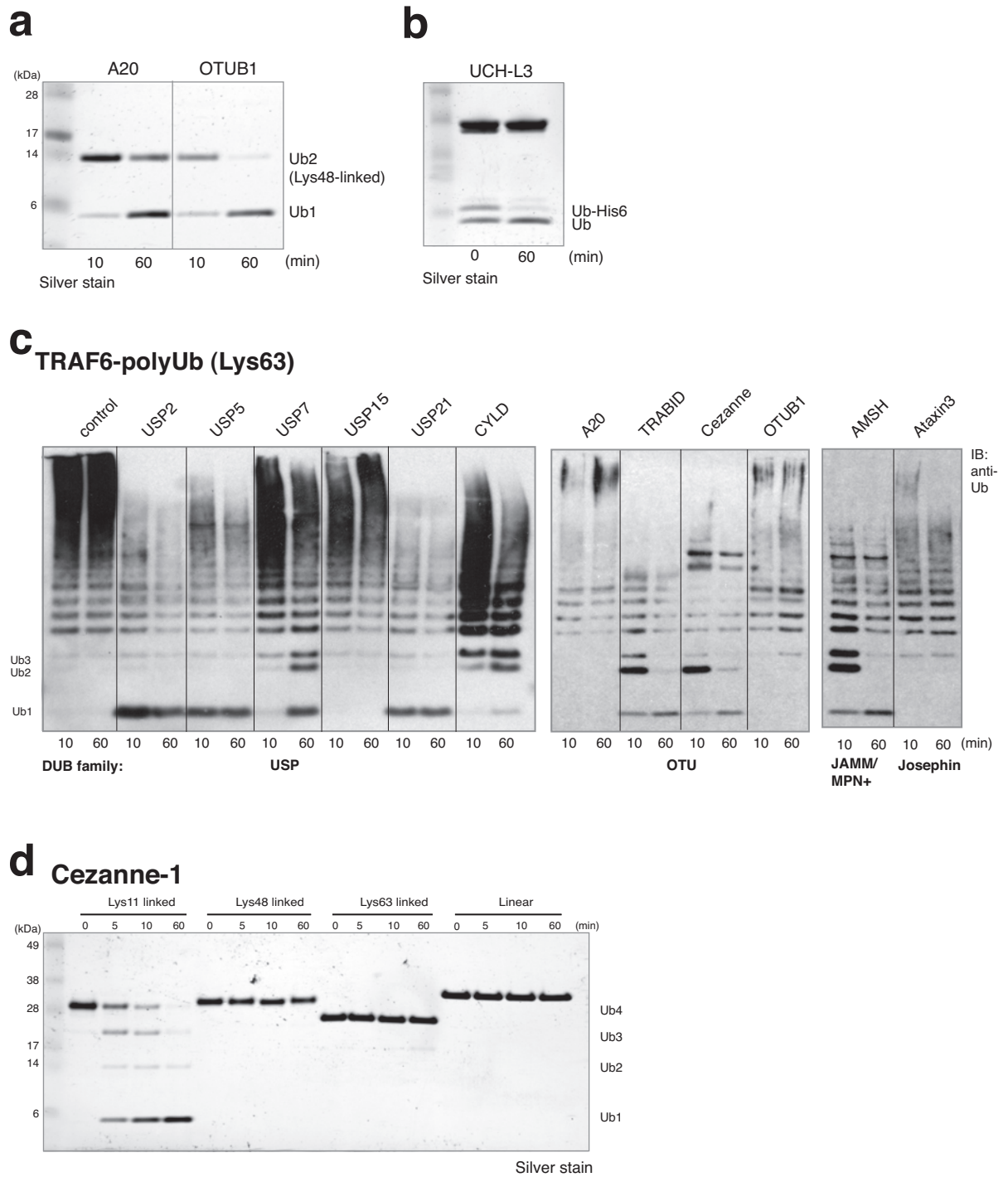
b Distal interface



Supplementary Figure 7: Differences between the asymmetric Lys11-diubiquitin interface in the crystals and in solution.

(a) Comparison of the proximal Lys11-linked diubiquitin interface in a view indicated by the arrow (left). Surface map of interacting residues from NMR (middle, orange, with shifting residues in blue, and Pro residues in yellow) and from the crystal interaction (right, yellow with interface residues in marine, according to the PISA server, www.ebi.ac.uk/pdbe/prot_int/pistart.html). (b) Comparison of the distal K11 diubiquitin interface, coloured as in (a), as viewed indicated by the arrow in the left picture. The 2nd image shows perturbed residues obtained from the distally labeled sample, and the third image from the fully labeled diubiquitin. The fourth image corresponds to the crystal structure interface. Two residues, Gly53 and Asp24, remain exchange broadened as in monomeric ubiquitin (white surface) indicating that this region of the interface is dynamic and can adopt multiple conformations. Similar observations of exchange broadening in interface residues have been made in the distal moiety of Lys48-linked diubiquitin molecule¹⁸. However, two further residues that reside on the distal interface of the crystal structure, Asp39 and Asp52 are also unperturbed in solution (circled), suggesting that the distal side of the interface moves or rotates slightly, in comparison to the conformation observed in the crystal structure.

Supplementary Figure 8



Supplementary Figure 8: Further controls for the DUB assays and activity against Lys63-polyubiquitinated TRAF6.

(a) Hydrolysis of Lys48-linked diubiquitin by A20 and OTUB1 and (b) cleavage of the C-terminal His-tag in ubiquitin-His6 by UCH-L3 confirms enzyme activity. (c) The panel of DUBs was analyzed against Lys63-polyubiquitinated GST-TRAF6. See **Experimental Procedures** for further information. (d) Adjusted time course analysis for Cezanne1 as in **Fig. 7c** to resolve generation of Lys11-linked tri- and diubiquitin species at 5 min.

Supplementary Table 1: Concentration and origin of DUBs used in Fig. 6

DUB	Construct	Concentration used	Obtained from
USP2	USP2 Catalytic Domain	1.7 μ M	Enzo Life Sciences (BML-UW9850)
USP5 (IsoT)	USP5 long form	696 nM	Enzo Life Sciences (BML-UW9690)
USP7	His6-USP7 full-length	520 nM	BostonBiochem (E-519)
USP 15	His6-USP15 full-length	593 nM	Enzo Life Sciences (BML-UW9845)
USP 21	Catalytic USP domain	160 nM	(Yu Ye and DK, unpublished)
CYLD	Catalytic USP domain	1.5 μ M	5
A20	Catalytic OTU domain	1.6 μ M	6
TRABID	Catalytic OTU domain	1.3 μ M	3
Cezanne	Catalytic OTU domain	67 nM	(this manuscript)
OTUB1	Full length	2.1 μ M	7
AMSH	Full length	1.3 μ M	8
Ataxin 3	Full length	1.6 μ M	9
UCH-L1	Full length	2.7 μ M	Enzo Life Sciences (BML-UW9740)
UCH-L3	Full-length	2.6 μ M	10

Supplementary Discussion

Structural insights into longer Lys11-linked chains

As mentioned in the main text, 12 ubiquitin molecules were present in the asymmetric unit, forming 6 equivalent, Lys11-isopeptide-linked diubiquitin molecules (**Fig. 5**). In the crystal, each Lys11-linked diubiquitin molecule forms equivalent interactions with a second diubiquitin molecule, resulting in a planar, wheel-shaped arrangement with pseudo four-fold symmetry (**Supp. Fig. 4a, b**). These four ubiquitin molecules interact through equivalent asymmetric interfaces (**Supp. Fig. 4**) and all four molecules show connecting electron density at their Lys11 side chain, forming a circular entity (**Supp. Fig. 4a,b**). Hence, this represents an averaged mixture of parallel ubiquitin dimers across the lattice, resulting in linkage ambiguity (**Supp. Fig. 4c**). Eleven of twelve ubiquitin molecules in the asymmetric unit show this linkage ambiguity, which occurs similarly in other polyubiquitin structures ^{3,11}.

The highest-order structure in the Lys11-diubiquitin crystal is formed by the symmetric stacking of two ubiquitin tetramers, forming an octameric barrel-shaped structure (**Supp. Fig. 5**). The asymmetric unit contains one octameric 'barrel' and one 'half-barrel' that is completed by crystallographic symmetry operations (**Supp. Fig. 5a**). In these additional interactions between tetramers, each ubiquitin molecule interacts symmetrically (two-fold symmetry) with one ubiquitin in the adjacent tetramer. It is important to note that the Ile44 residues in the barrel-like structures are exposed to solvent, creating a hydrophobic surface on the outer rim of the barrel.

Closer analysis of the 'stacking' interactions reveals that the interface is symmetric and involves Val70 and Leu8 (**Supp. Fig. 5b**). More importantly, the linkage residues Lys11 and Gly76 are in close proximity. Although no linking electron density is observed for any 'stacking' ubiquitin interaction, a linkage seems feasible (**Supp. Fig. 5b**). Hence, the Lys11 side chain of each ubiquitin can be linked via an asymmetric interface (Lys29, Lys33) to a neighboring ubiquitin, or via a symmetric interface (Val70, Leu8) to a 'stacking' ubiquitin (**Supp. Fig.**

5b). It is a possibility that the NMR analysis represents a mixture of both conformations (**Supp. Fig. 5c**).

Hence, the crystal packing may suggest a model for higher-order oligomers of Lys11-linked ubiquitin chains. The observed differences between NMR and crystallographic dimers (**Fig. 4d, Supp. Fig 7**) indicate however that in solution, Lys11-linked ubiquitin chains may also adopt more open conformations.

Supplementary Experimental Procedures

Plasmids and constructs

GST-tagged full-length human UBE2S and UBE2C were a gift from Philip Cohen (Dundee), and truncations and catalytic mutants were performed by PCR and site-directed mutagenesis, respectively. Cezanne-1 was cloned from IMAGE cDNA obtained from Imagenes (Germany), and USP21 was cloned from a plasmid kindly provided by Sylvie Urbe (Liverpool). Expression constructs for OTUB1, Ataxin3 and UCH-L3 were kindly provided by Benedikt Kessler (Oxford), Sokol Todi (Ann Arbor, USA), and Keith D. Wilkinson (Atlanta, USA), respectively.

Expression and purification of recombinant proteins

Recombinant GST-fusion proteins were expressed in Rosetta 2 (DE3) pLacI cells (Novagen). 1 L cultures of cells were induced at OD₆₀₀ of 0.6 with 250 μ M IPTG and proteins were expressed at 20 °C overnight. Cells were harvested and flash-frozen. 30 ml lysis buffer (270 mM sucrose, 50 mM Tris (pH 8.0), 50 mM NaF, 1 protease inhibitor cocktail tablet (Roche), 0.1 % (v/v) β -mercaptoethanol, 1 mg ml⁻¹ lysozyme, 0.1 mg ml⁻¹ DNase) was added per liter of culture. After sonication, cell lysates were cleared by centrifugation using a Sorvall SS-34 rotor (18,000 rpm, 30 min, 4 °C) and supernatants were incubated with Glutathione Sepharose 4B (GE Healthcare) for 1 h to immobilize soluble GST fusion proteins. Subsequently, the sepharose beads were washed with 500 ml high salt buffer [500 mM NaCl, 25 mM Tris (pH 8.5), 5 mM DTT] and 300 ml low salt buffer [150

mM NaCl, 25 mM Tris (pH 8.5), 5 mM DTT]. For site-specific cleavage of the GST tag, immobilized fusion proteins were incubated with 30 mM PreScission protease (GE Healthcare) overnight. Cleaved proteins were eluted with low salt buffer and flash-frozen in liquid nitrogen. All samples were >95% pure after purification.

Mass spectrometry

LC-MS/MS was carried out by nanoflow reverse phase liquid chromatography (using a U3000 from Dionex) coupled online to a Linear Ion Trap (LTQ)-Orbitrap XL mass spectrometer (Thermo Scientific). Briefly, the LC separation was performed using a C18 PepMap capillary column (75 μ m ID \times 150 mm; Dionex) and the peptides were eluted using a linear gradient from 5 % (v/v) B to 50 % (v/v) B over 40 minutes at a flow rate of 200 nL min⁻¹ (solvent A: 98 % H₂O; 2 % (v/v) acetonitrile in 0.1% (v/v) formic acid; solvent B: 90 % (v/v) acetonitrile in 0.1 % (v/v) formic acid). The eluted peptides were electrosprayed into the mass spectrometer via a nanoelectrospray source fitted with a PicoTip emitter (New Objective). A cycle of one full FT scan mass spectrum (350-2000 m/z, resolution of 60 000 at m/z 400) was followed by 6 data-dependent MS/MS acquired in the linear ion trap with normalized collision energy (setting of 35 %). Target ions already selected for MS/MS were dynamically excluded for 60 s. Peptides were identified from MS/MS spectra by searching against a Swissprot database using the Mascot search algorithm (www.matrixscience.com) and Proteome Discoverer (Thermo Fisher Scientific). Oxidation of methionine, GlyGly and LeuArgGlyGly addition on Lysine residues were used as variable modifications. Initial mass tolerance was set to 10 ppm for peptide parent mass, 0.8 Da for fragment masses and enzyme restriction was set to trypsin specificity with 2 missed cleavages.

Supplementary References

1. Adams, P.D. et al. PHENIX: building new software for automated crystallographic structure determination. *Acta Crystallogr D Biol Crystallogr* **58**, 1948-54 (2002).
2. Cook, W.J., Jeffrey, L.C., Carson, M., Chen, Z. & Pickart, C.M. Structure of a diubiquitin conjugate and a model for interaction with ubiquitin conjugating enzyme (E2). *J Biol Chem* **267**, 16467-71 (1992).
3. Komander, D. et al. Molecular discrimination of structurally equivalent Lys 63-linked and linear polyubiquitin chains. *EMBO Rep* **10**, 466-73 (2009).
4. Varadan, R., Walker, O., Pickart, C. & Fushman, D. Structural properties of polyubiquitin chains in solution. *J Mol Biol* **324**, 637-47 (2002).
5. Komander, D. et al. The structure of the CYLD USP domain explains its specificity for Lys63-linked polyubiquitin and reveals a B box module. *Mol Cell* **29**, 451-64 (2008).
6. Komander, D. & Barford, D. Structure of the A20 OTU domain and mechanistic insights into deubiquitination. *Biochem J* **409**, 77-85 (2008).
7. Edelmann, M.J. et al. Structural basis and specificity of human otubain 1-mediated deubiquitination. *Biochem J* **418**, 379-90 (2009).
8. McCullough, J., Clague, M.J. & Urbé, S. AMSH is an endosome-associated ubiquitin isopeptidase. *J Cell Biol* **166**, 487-92 (2004).
9. Winborn, B.J. et al. The deubiquitinating enzyme ataxin-3, a polyglutamine disease protein, edits Lys63 linkages in mixed linkage ubiquitin chains. *J Biol Chem* **283**, 26436-43 (2008).
10. Johnston, S.C., Larsen, C.N., Cook, W.J., Wilkinson, K.D. & Hill, C.P. Crystal structure of a deubiquitinating enzyme (human UCH-L3) at 1.8 Å resolution. *Embo J* **16**, 3787-96 (1997).
11. Eddins, M.J., Varadan, R., Fushman, D., Pickart, C.M. & Wolberger, C. Crystal structure and solution NMR studies of Lys48-linked tetraubiquitin at neutral pH. *J Mol Biol* **367**, 204-11 (2007).

Supplementary Data

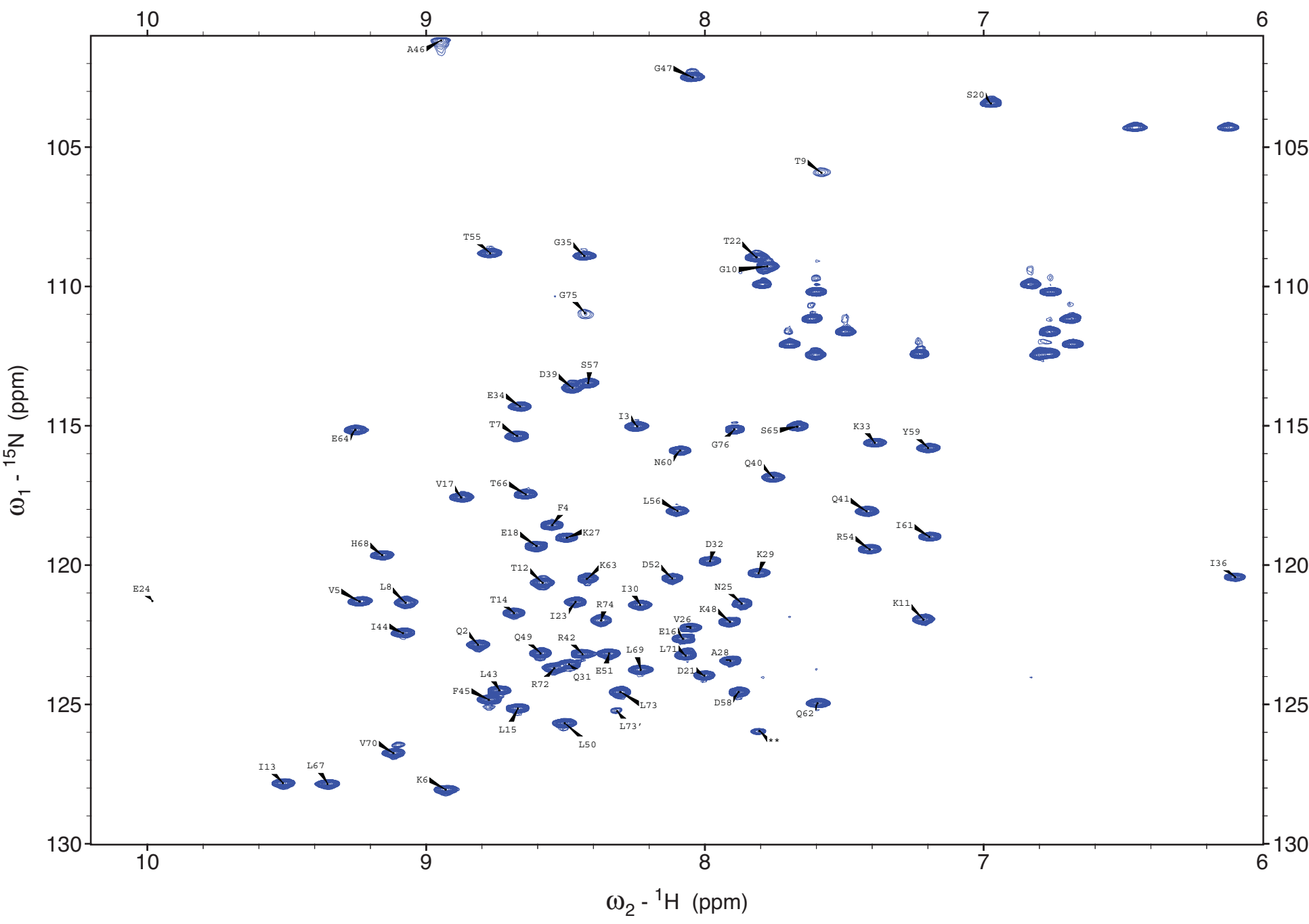
Reassigned NMR spectra 1-4: pH 7.2

Contributions from a minor population of a second conformer were observed for Val70 and Leu73 (marked with L73') in K63R monoubiquitin. No signal was observed for Gly53, and very weak cross-peaks for residues Thr9, Glu24 and Gly75 indicate substantial conformational exchange for these residues. Diubiquitin samples had a minor contamination with K11R or K63R monoubiquitin, respectively. In the case of non-overlapped signals, these are marked with *. The peak marked ** is most likely a folded signal of a side chain, no cross peaks were observed for these peaks in triple resonance experiments. No doubling of peaks was observed for K11R monoubiquitin. No signals were found for Gly53, and Thr9, Glu24 and Gly75 exhibit very weak cross peaks. In the uniformly labeled K63R diubiquitin sample, signals for residues with distinct chemical shift positions for the distal and/or proximal moiety are labeled with a suffix b or c.

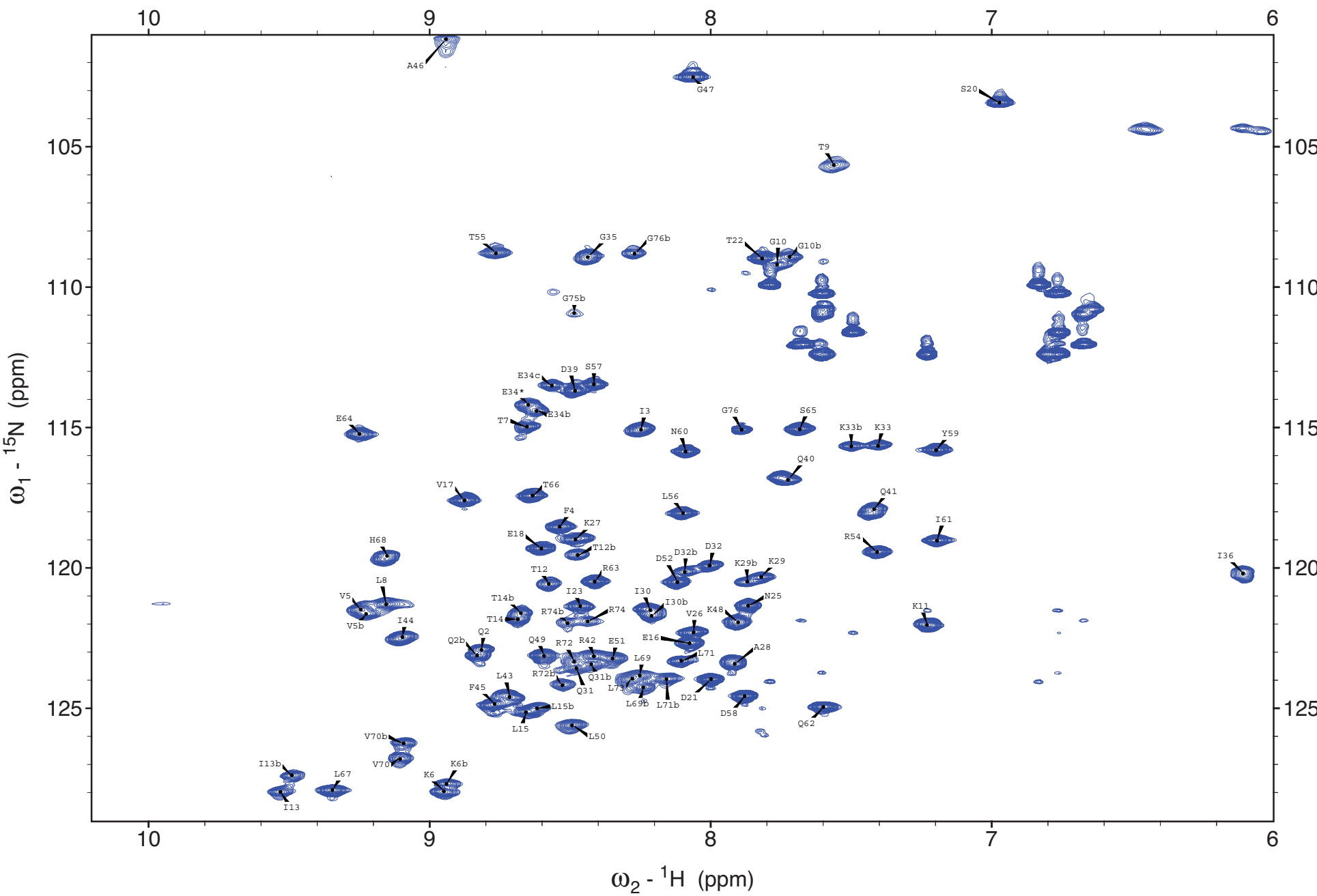
Reassigned NMR spectra 5-8: pH 3.5

Residues Val70, Leu71, Arg72 in K63R monoubiquitin exhibit two sets of signals most likely due to the presence of two conformations for these residues. No significant doubling of peaks was observed for K11R monoubiquitin or any of the diubiquitin samples. In the uniformly labeled K63R diubiquitin sample, signals for residues with distinct chemical shift positions for the distal and/or proximal moiety are labeled with a suffix b or c. Peak positions labeled with a suffix c are most likely from the distal moiety based on a comparison with the distal ^{13}C , ^{15}N -labeled K11R diubiquitin. Diubiquitin samples had a minor contamination with K11R or K63R monoubiquitin, respectively. In the case of non-overlapped signals, these are marked with *. Peaks marked ** are most likely folded side chain signals, no cross peaks were observed for these peaks in triple resonance experiments.

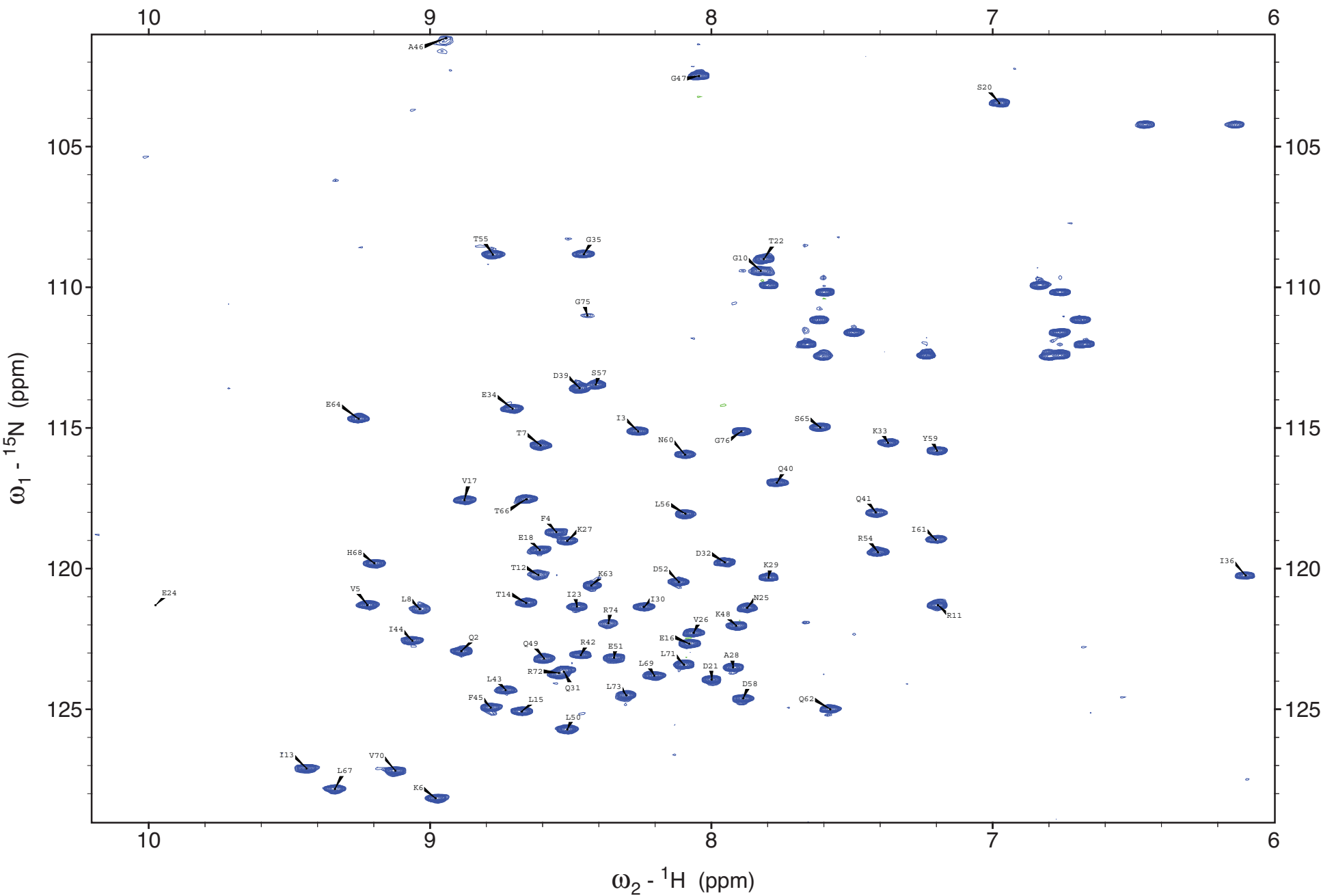
Spectrum 1 : Ub K63R , pH 7.2



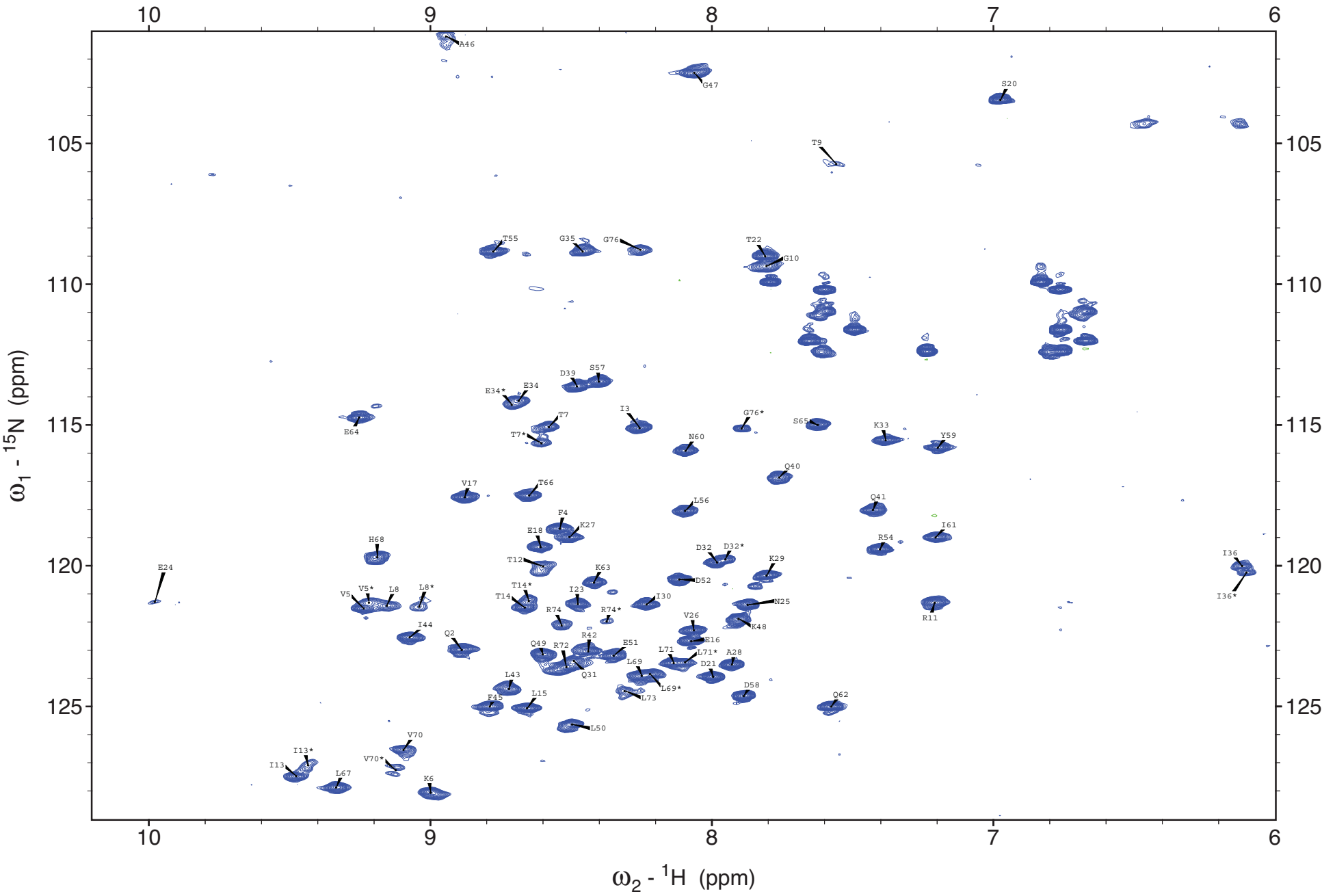
Spectrum 2 : K11-linked diUb K63R , pH 7.2



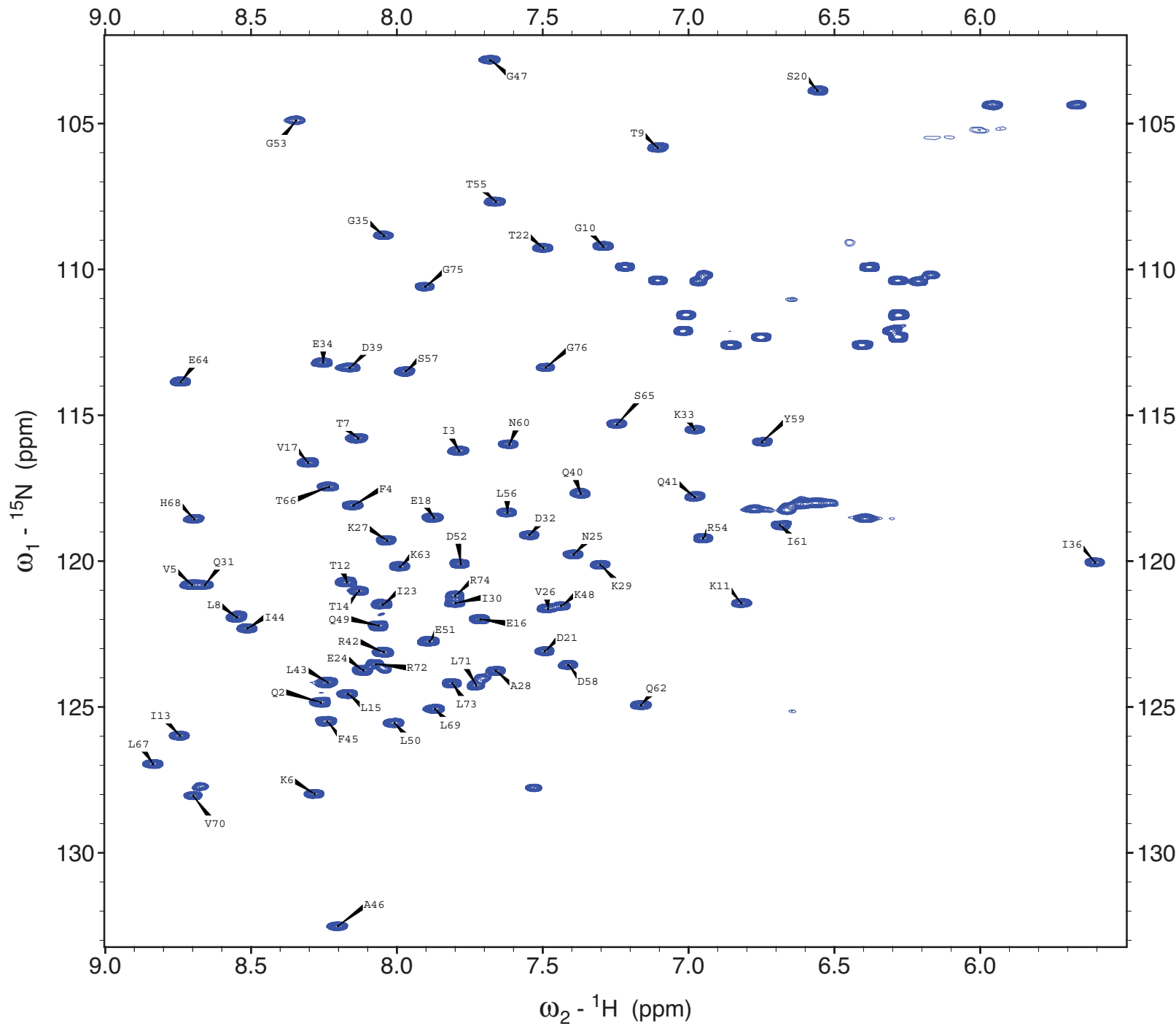
Spectrum 3 : Ub K11R , pH 7.2



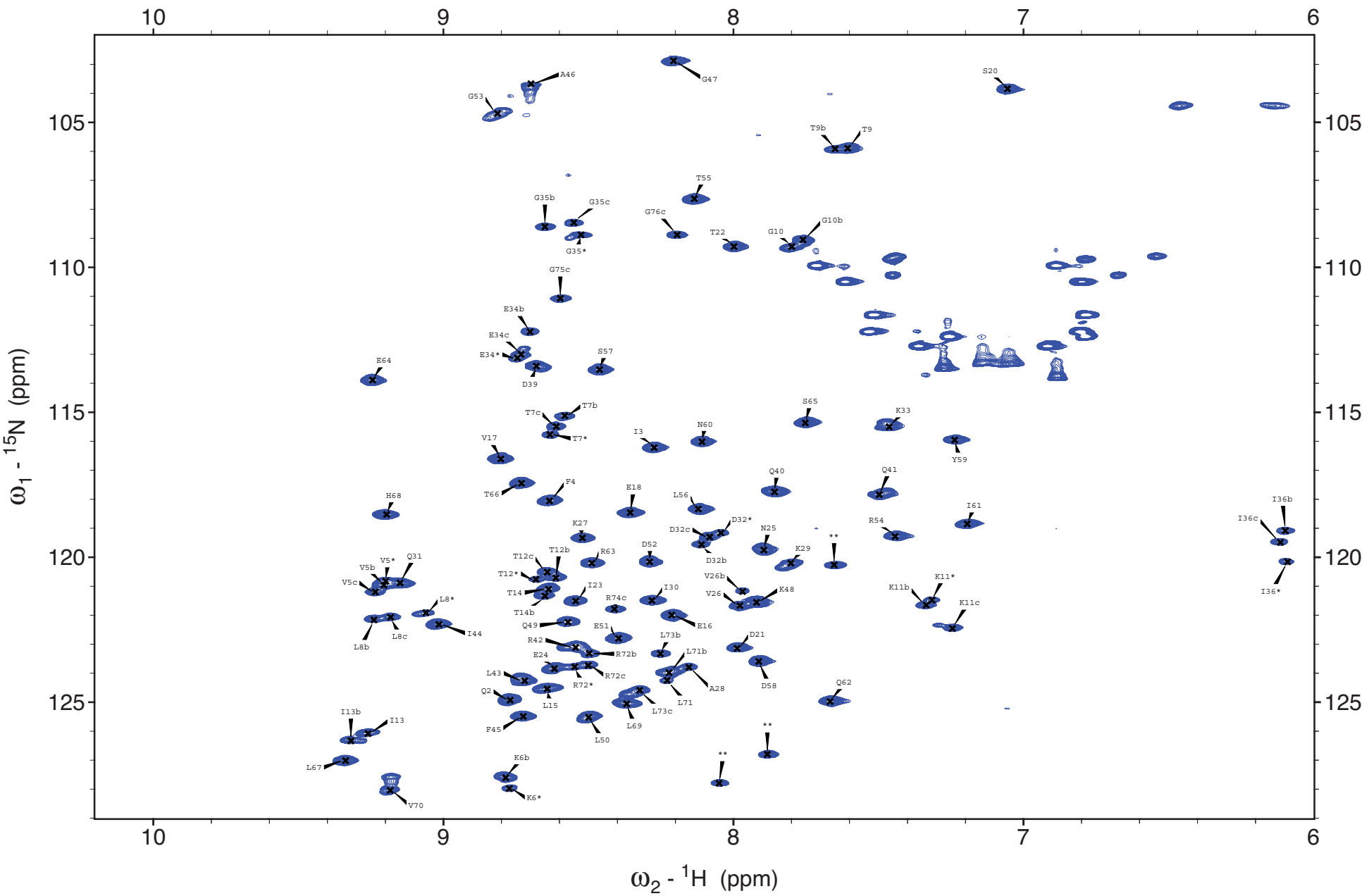
Spectrum 4 : distally labeled K11-linked diUb K11R , pH 7.2



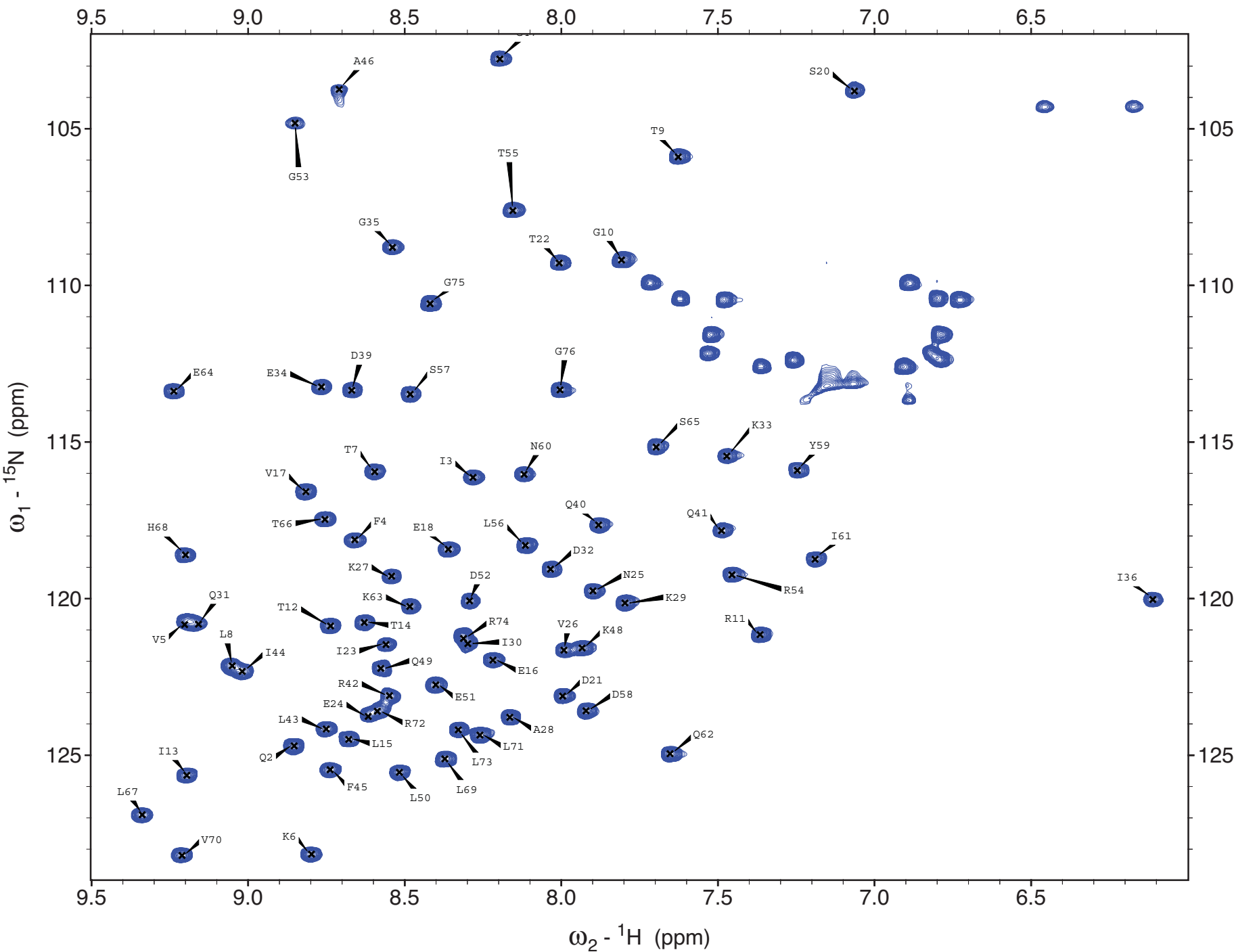
Spectrum 5 : Ub K63R , pH 3.5



Spectrum 6 : K11-linked diUb K63R , pH 3.5



Spectrum 7 : Ub K11R , pH 3.5



Spectrum 8 : distally labelled K11-linked diUb K11R , pH 3.5

